THE JOURNAL OF BIOLOGICAL CHEMISTRY VOL. 283, NO. 11, pp. 6668–6676, March 14, 2008

Direct Hemin Transfer from IsdA to IsdC in the Iron-regulated Surface Determinant (Isd) Heme Acquisition System of *Staphylococcus aureus*[*]

Received for publication, October 9, 2007, and in revised form, January 2, 2008 Published, JBC Papers in Press, January 9, 2008, DOI 10.1074/jbc.M708372200

Mengyao Liu[‡], Wesley N. Tanaka[‡], Hui Zhu[‡], Gang Xie[‡], David M. Dooley[§], and Benfang Lei[‡1]

From the Departments of [‡]Veterinary Molecular Biology and [§]Chemistry and Biochemistry, Montana State University, Bozeman, Montana 59718

The iron-regulated surface determinants (Isd) of *Staphylococcus aureus*, including surface proteins IsdA, IsdB, IsdC, and IsdH and ATP-binding cassette transporter IsdDEF, constitute the machinery for acquiring heme as a preferred iron source. Here we report hemin transfer from hemin-containing IsdA (holo-IsdA) to hemin-free IsdC (apo-IsdC). The reaction has an equilibrium constant of 10 ± 5 at 22 °C in favor of holo-IsdC formation. During the reaction, holo-IsdA binds to apo-IsdC and then transfers the cofactor to apo-IsdC with a rate constant of 54.3 ± 1.8 s^{-1} at 25 °C. The transfer rate is >70,000 times greater than the rate of simple hemin dissociation from holo-IsdA into solvent ($k_{transfer}$ = 54.3 s^{-1} *versus* k_{-hemin} = 0.00076 s^{-1}). The standard free energy change, ΔG^0, is −27 kJ/mol for the formation of the holo-IsdA-apo-IsdC complex. IsdC has a higher affinity for hemin than IsdA. These results indicate that the IsdA-to-IsdC hemin transfer is through the activated holo-IsdA-apo-IsdC complex and is driven by the higher affinity of apo-IsdC for the cofactor. These findings demonstrate for the first time in the Isd system that heme transfer is rapid, direct, and affinity-driven from IsdA to IsdC. These results also provide the first example of heme transfer from one surface protein to another surface protein in Gram-positive bacteria and, perhaps most importantly, indicate that the mechanism of activated heme transfer, which we previously demonstrated between the streptococcal proteins Shp and HtsA, may apply in general to all bacterial heme transport systems.

Bacterial pathogens have evolved acquisition machinery for heme as a preferred source of essential iron. In Gram-negative pathogens, specific outer membrane receptors (1, 2) sequester heme from heme-hemophore complexes or host hemoproteins and bring it into the periplasmic space in a TonB-dependent process (3). Specific ATP-binding cassette (ABC)[2] transporters then transport heme across the cytoplasmic membrane (4). A heme-specific ABC transporter is also a component of the heme acquisition machinery in Gram-positive pathogens such as *Corynebacterium diphtheriae* (5), *Streptococcus pyogenes* (6, 7), *Staphylococcus aureus* (8), and *Streptococcus equi* (9). In addition, cell surface heme-binding proteins have been identified in *S. pyogenes* (10), *S. aureus* (11), *S. equi* (9), and *Bacillus anthracis* (12), suggesting that, besides ABC transporters, cell surface heme-binding proteins are required for heme acquisition by Gram-positive bacteria.

The *S. aureus* heme uptake system consists of the iron-regulated surface determinants (Isd), including the surface proteins IsdA, IsdB, IsdH or HarA, and IsdC, and ABC transporters IsdDEF and HtsABC (8, 11). The *S. pyogenes* heme uptake machinery consists of the surface proteins, Shr and Shp, and ABC transporter HtsABC (6, 7, 10, 13–16). The surface protein components, Shr and Shp of the GAS acquisition machinery and IsdA, IsdB, IsdH, and IsdC of the *S. aureus* system, do not share significant sequence homology. Thus, the *S. pyogenes* and *S. aureus* systems represent two distinct heme acquisition pathways in Gram-positive bacteria. The *S. pyogenes* system has a homologue in *S. equi* (9), whereas the homologue of the *S. aureus* system is present in *B. anthracis* (12). These surface proteins, but not Shp, contain the NEAr transporter (NEAT) domains (17), although the structure of the Shp heme-binding domain (18) is similar to that of the NEAT domains of IsdA (19) and IsdC (20).

Previous characterization of the Isd system from *S. aureus* indicated that the system takes up hemin as an iron source (11). IsdB is a hemoglobin receptor and is required for uptake of hemin from methemoglobin (21). IsdH binds haptoglobin-hemoglobin, although it appears not to be critical for using methemoglobin hemin as an iron source *in vitro* (22). IsdA and the *B. anthracis* homologue of IsdC are also important for hemin uptake (12, 19). IsdB, IsdA, and IsdC bind heme (11, 19, 20, 23, 24), and structural studies show that IsdA and IsdC bind hemin in a pentacoordinate complex with a tyrosine residue as the only axial ligand (19, 20), in contrast to the hexacoordination of the heme iron in Shp and HtsA (14, 15). It has been proposed that IsdH and IsdB capture haptoglobin-hemoglobin and hemoglobin, respectively, and heme is transferred from bound

[*] This work was supported in part by National Center for Research Resources Grant P20 RR-020185 (to B. L.), National Institutes of Health Grant GM27659 (to D. M. D.), United States Department of Agriculture Grant NRI/CSREES 2007-35204-18306, Formula Funds and the Montana State University Agricultural Experimental Station, and National Science Foundation Research Experience Undergraduates Program Grant DBI-0453021 (to A. Metz). The costs of publication of this article were defrayed in part by the payment of page charges. This article must therefore be hereby marked "*advertisement*" in accordance with 18 U.S.C. Section 1734 solely to indicate this fact.

[1] To whom correspondence should be addressed: Dept. of Veterinary Molecular Biology, Montana State University, P. O. Box 173610, Bozeman, MT 59717. Tel.: 406-994-6389; Fax: 406-994-4303; E-mail: blei@montana.edu.

[2] The abbreviations used are: ABC, ATP-binding cassette; Isd, iron-regulated surface determinants; NEAT, NEAr transporter.

hemoglobin to IsdA, then IsdC, and finally to ABC transporters IsdDEF and/or HtsABC (25, 26). This hypothesis has not been experimentally tested, and little is known about the biochemical mechanism of heme acquisition by this system. This study describes the rapid and direct hemin transfer from holo-IsdA to heme-free IsdC (apo-IsdC). This affinity-driven transfer occurs in two steps, the formation of a holo-IsdA-apo-IsdC complex and subsequent hemin transfer. This study not only unveils the first hemin transfer reaction of the Isd system but also documents the first example of hemin transfer from one surface protein to another surface protein in Gram-positive bacteria.

EXPERIMENTAL PROCEDURES

Gene Cloning—The *isdA* and *isdC* genes were PCR-cloned from *S. aureus* subsp. *aureus* MW2 using paired primers 5′-TACCATGGACAGCCAACAAGTCAATGCG-3′/5′-TGAA-TTCTTAAGTTTTTGGTAATTGTTTAGC-3′ and 5′-ACC-ATGGATAGCGGTACTTTGAATTATG-3′/5′-AGAATTC-TTATGTTTGTGGATTTTCTACTTTGTC-3′, respectively. The *isdA* and *isdC* PCR products were digested with NcoI/EcoRI and cloned into pET-His2 (6) at the same sites, yielding pISDA and pISDC. Recombinant IsdA and IsdC proteins produced from the constructs had 11 amino acid residues (MHH-HHHHLETM) fused to Asp-30 and Asp-40, respectively, and lacked their transmembrane domain and charged tail at the C terminus (amino acids 317–350 and 193–227 for IsdA and IsdC, respectively). Both gene clones were sequenced to rule out spurious mutations.

Protein Purification—Both IsdA and IsdC were expressed in *Escherichia coli* BL21 (DE3) containing pISDA and pISDC, respectively. Bacteria were grown at 37 °C in 6 liters of Luria-Bertani broth supplemented with 100 mg/liter ampicillin to an absorbance at 600 nm of about 1.0, and the production of the proteins were induced by 0.4 mM isopropyl β-D-thiogalactopyranoside for 6 h. Bacteria were harvested by centrifugation. The bacterial pellet was suspended in 60 ml of 20 mM Tris-HCl, pH 8.0, and sonicated on ice for 15 min. IsdA and IsdC in the lysate were purified according to the manufacturer's protocol using a nickel-nitrilotriacetic acid-agarose column.

Preparation of Apo-IsdA and Apo-IsdC—Purified recombinant IsdC was a mixture of apo-form and a complex with iron-free protoporphyrin. To prepare apo-IsdC, the mixture in 20 mM Tris-HCl, pH 8.0, was loaded onto a DEAE-Sepharose column (1.5 × 5 cm). Apo-IsdC was eluted with 30 mM NaCl in Tris-HCl, dialyzed against 3 liters of Tris-HCl. Apo-IsdA was prepared using the methyl ethyl ketone method (27).

Preparation of Holo-IsdA and Holo-IsdC—Holo-IsdC was obtained by reconstitution of its apo-form with hemin. One ml of apo-IsdC was incubated with excess hemin, loaded onto a Sephadex G-25 column (0.5 × 30 cm), and eluted with 10 mM Tris-HCl, pH 8.0. The holoprotein without free hemin was collected. Purified IsdA was a mixture of apo- and holo-forms. Homogeneous holo-IsdA was similarly prepared by reconstituting apo-IsdA in the mixture with hemin.

Determination of Protein Concentration and Heme Content—Protein concentration was determined using a modified Lowry protein assay kit purchased from Pierce with bovine serum albumin as a standard. Heme content was measured using the pyridine hemochrome assay with the extinction coefficient ϵ_{418} = 191.5 mM^{-1} cm^{-1} (28).

Rates of Hemin Association to and Dissociation from IsdA and IsdC—The rates of hemin dissociation from holo-IsdA and holo-IsdC were measured using H64Y/V68F whale sperm apomyoglobin as a hemin scavenger according to the previous method (29) with slight modification. Each protein (3 μM) was incubated with 48 μM apomyoglobin in 1 ml of 20 mM Tris-HCl, pH 8.0, and the changes in absorbance at 600 and 554 nm were monitored. Sucrose in the original method was not used in this study. The $\Delta(A_{600}-A_{554})$ time courses were fit to a single exponential equation to obtain the first-order rate constants for hemin dissociation.

The rates of hemin binding to the apoproteins were measured using a stopped-flow spectrophotometer equipped with a photodiode array detector (SX20; Applied Photophysics). Hemin (2 μM) in one syringe was mixed with apoprotein at ≥3 times [hemin] in another syringe. Entire spectra were recorded over time in each reaction. Changes in absorbance at the indicated wavelengths were analyzed as described under "Results."

Hemin Transfer—Holo-IsdA and apo-IsdC or holo-IsdC and apo-IsdA at indicated concentrations were incubated in 0.1 ml of 20 mM Tris-HCl, pH 8.0, at room temperature (22 °C) for 2 or 20 min. Each mixture was then loaded onto a small DEAE-Sepharose column (0.2 ml of resin), and the column was first eluted with 0.3 ml Tris-HCl to recover IsdA, which did not bind to the column, and then washed with 1 ml of Tris-HCl. IsdC bound to the column was eluted with 0.3 ml of 0.2 M NaCl in Tris-HCl. Separation of the two proteins was confirmed by SDS-PAGE analysis. The concentrations of holo-IsdA and holo-IsdC in the isolated samples were calculated from A_{406} using the extinction coefficients of 9.5×10^4 and 1.1×10^5 $M^{-1}{\cdot}cm^{-1}$, respectively. The concentrations of apo-IsdA and apo-IsdC in the same samples were calculated from A_{280} after subtracting the contribution from the holo-form using the extinction coefficients of 1.6×10^4 and 1.8×10^4 $M^{-1}{\cdot}cm^{-1}$, respectively.

Kinetics of Hemin Transfer from Holo-IsdA to Apo-IsdC—The spectral changes associated with hemin transfer from holo-IsdA to apo-IsdC were used to measure the transfer rate using the stopped-flow spectrophotometer at the indicated temperatures. Holo-IsdA (2.4 μM) in one syringe was mixed with apo-IsdC at >5 times [holo-IsdA] in another syringe. Entire spectra were recorded over a range of 250 – 800 nm against time in each reaction. Changes in absorbance at the appropriate wavelengths were analyzed.

RESULTS

IsdA and IsdC Proteins—Purified recombinant IsdA was a mixture of apo- and holo-forms. Homogeneous holo-IsdA was prepared by reconstitution of apo-IsdA with hemin, and 95% apo-IsdA was prepared by extraction with methyl ethyl ketone. Holo-IsdA exhibits absorption peaks at 406, 503, 529, and 622 nm in the visible region (Fig. 1*A*). Reduction of holo-IsdA with dithionite shifted the Soret peak from 406 to 430 nm and abolished the A_{622} peak but did not result in the resolved α and β absorption bands seen in hemochrome (Fig. 1*A*). These absorp-

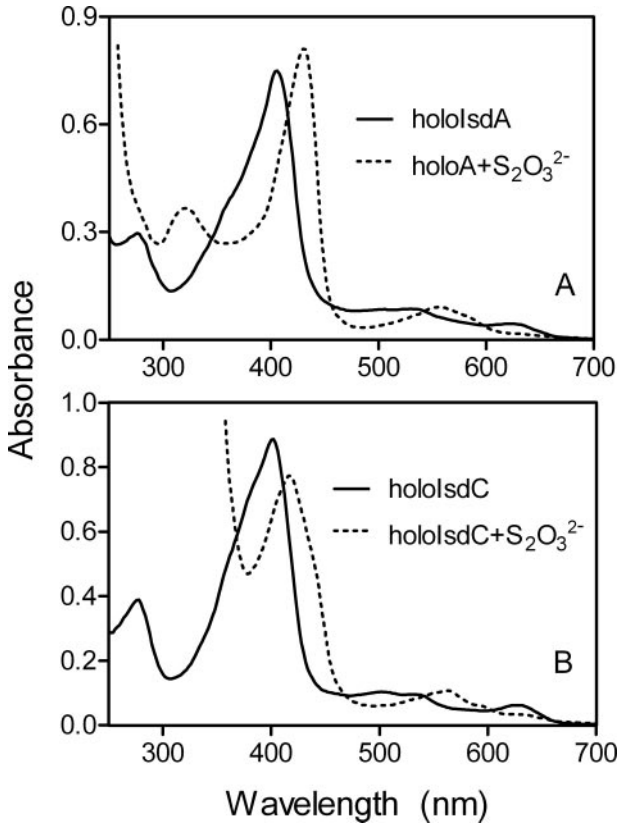

FIGURE 1. **Optical absorption spectra of oxidized and reduced IsdA (*A*) and IsdC (*B*) each at 8 μM.** The reduced spectra were recorded in the presence of excess dithionite.

tion features are consistent with the previous observation that the heme iron in IsdA is pentacoordinate (19, 24).

Purified recombinant IsdC was also a mixture of apoprotein and a complex that displays absorption peaks at 407, 511, 547, 570, and 625 nm (data not shown) in the visible region. This feature is almost identical to that of the GST-IsdC fusion protein, which was found to bind iron-free protoporphyrin (23), indicating that the chromophore associated with IsdC was protoporphyrin. Apo-IsdC was readily separated from the IsdC-protoporphyrin complex by anion exchange chromatography. Holo-IsdC reconstituted from apo-IsdC and hemin displays the broad Soret peak at 402 nm and charge transfer bands at 501, 532, and 626 nm (Fig. 1*B*). Holo-IsdC treated with dithionite possesses the Soret peak at 417 nm and lacks the dominant α and β bands, and the reduction of holo-IsdC appears not to be complete (Fig. 1*B*). These spectral characteristics are consistent with the pentacoordination of the heme iron in the crystal structure of IsdC (20).

Relative Affinity of IsdA and IsdC for Hemin—To determine the affinity of IsdA for hemin, the rates of hemin binding and dissociation from IsdA were measured. When hemin was mixed with apo-IsdA, the spectrum of the reaction shifted from that of free hemin to those of holo-IsdA (Fig. 2*A*). The time course of $\Delta(A_{406}-A_{374})$ could be described by a two-exponential equation, resulting in two observed rate constants. The fast and slow phases contributed to approximate 70 and 30% of the total spectral change, respectively (Fig. 2*C*). The value of observed rate constant in the fast phase (k_{obs1}) varies hyperbolically with [apo-IsdA], whereas the observed rate constant in the slow phase (k_{obs2}) does not display a clear dependence on [apo-IsdA] (Fig. 2*D*). Using the method of de Villiers *et al.* (30), monomeric Fe(III)-protoporphyrin IX was ~60% of total hemin at 2 μM in 20 mM Tris-HCl, pH 8.0. Thus, the fast phase is most likely the reaction of apo-IsdA with monomeric hemin. If this is true, the results of the fast-phase reaction suggest a two-step binding process involving the formation of a hemin-apoprotein intermediate that is followed by axial coordination to form the final holoprotein as proposed in Scheme 1, where k_1 and k_2 are the rate constants for bimolecular formation and unimolecular dissociation of the initial apoprotein-hemin complex, respectively, and $k_{coordination}$ and k_{-hemin} are the internal first-order rate constants for iron coordination to and dissociation from the final protein ligands, respectively.

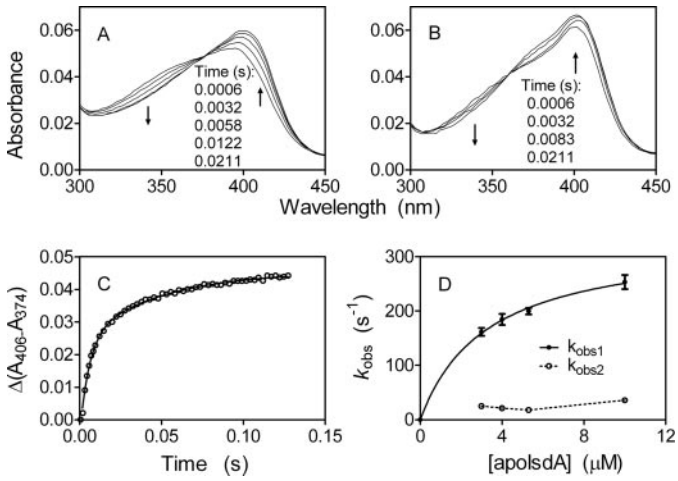

FIGURE 2. **Hemin association to apo-IsdA and apo-IsdC.** *A* and *B*, spectral shifts over time in the reactions of 1.0 μM hemin with 10 μM apo-IsdA (*A*) or 3.9 μM apo-IsdC (*B*). *C*, time courses of $\Delta(A_{406}-A_{374})$ in *A*. The *symbol and curve* are the observed data and two-exponential fitting curve, respectively. *D*, observed rate constants of the fast (k_{obs1}) and slow (k_{obs2}) phases for hemin binding to apo-IsdA as a function of [apo-IsdA]. The *curve* for k_{obs1} is a theoretical line obtained by fitting the data to Equation 1.

If k_1 and k_2 are much greater than $k_{coordination}$, and k_{-hemin} is much smaller than $k_{coordination}$, the observed constant in the fast phase (k_{obs1}) is described by Equation 1,

$$k_{obs1} = \frac{k_{coordination}[apoprotein]}{k_2/k_1 + [apoprotein]} = \frac{k_{coordination}[apoprotein]}{K_d + [apoprotein]} \quad \text{(Eq. 1)}$$

where K_d is k_2/k_1. The values for K_d and $k_{coordination}$ from fitting the k_{obs1} data in Fig. 2*D* to Equation 1 are 3.3 ± 0.7 μM and 330 ± 27 s^{-1}, respectively. At low apoprotein concentrations where the reaction appears bimolecular, the apparent second-order rate constant ($k_{coordination}/K_d$) is 100 $\mu M^{-1}\cdot s^{-1}$.

To determine the rate of dissociation of hemin from IsdA, IsdA was mixed with excess H64Y/V68F apomyoglobin, and dissociated hemin was captured by apomyoglobin. At 6 h after mixing holo-IsdA and apo-Mb, the mixture displayed the spectrum of H64Y/V68F holomyoglobin, as evidenced by the formation of the A_{600} peak (Fig. 3*A*), indicating the loss of hemin from IsdA. $\Delta(A_{600}-A_{544})$ time course associated with the hemin dissociation was fitted to a single exponential

$$\text{Hemin} + \text{apoprotein} \underset{k_2}{\overset{k_1}{\rightleftharpoons}} \text{hemin:apoprotein} \underset{k_{\text{-hemin}}}{\overset{k_{coordination}}{\rightleftharpoons}} \text{holoprotein}$$

$$k'_{\text{hemin}} = \frac{k_{\text{coordination}}}{k_2/k_1} \qquad K_{\text{hemin}} = \frac{k_1 k_{\text{coordination}}}{k_2 k_{-\text{hemin}}} = \frac{k'_{\text{hemin}}}{k_{\text{-hemin}}}$$

SCHEME 1

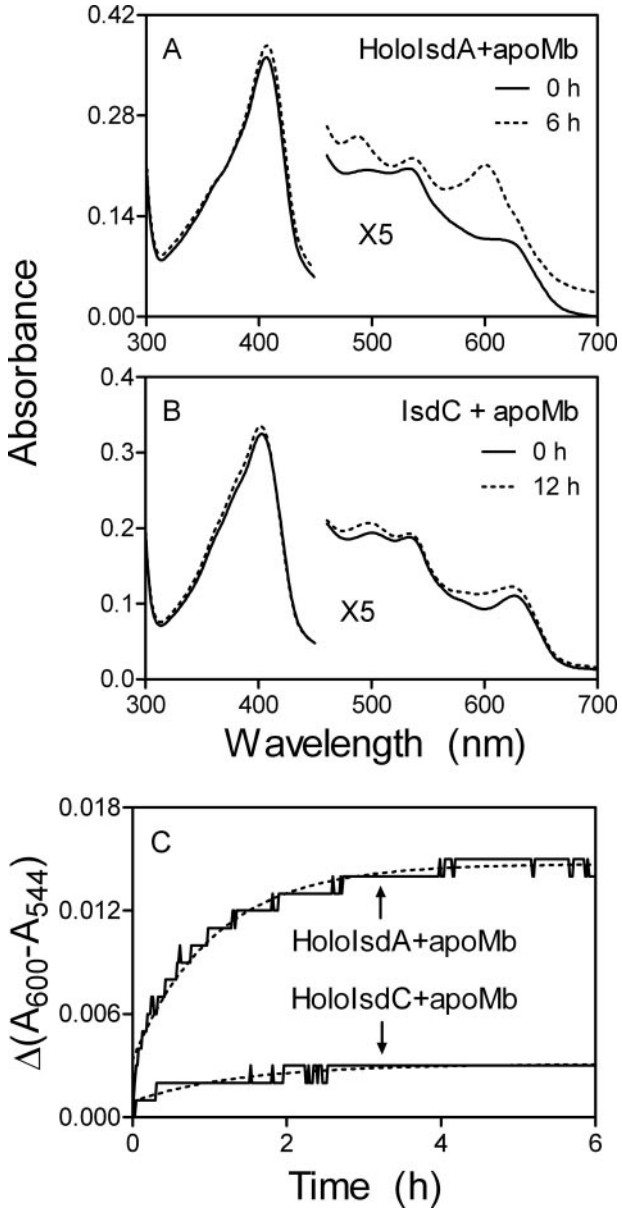

FIGURE 3. **Dissociation of hemin from IsdA and IsdC.** Holo-IsdA or holo-IsdC at 3 μM was incubated with 48 μM H64Y/V68F apomyoglobin in 20 mM Tris-HCl, pH 8.0, at 25 °C. *A* and *B*, spectra of the mixture at 0 and 6 or 12 h after mixing. *C*, time courses of $\Delta(A_{600}-A_{544})$ in these reactions of hemin dissociation. The *dashed lines* are the theoretical curves obtained by fitting the data to a single exponential equation.

equation (Fig. 3*C*), obtaining $k_{-\text{hemin}}$ of 0.95 ± 0.02 h^{-1}. Because the dissociation of hemin is extremely slow, $k_{-\text{hemin}}$ in Scheme 1 must be $\ll k_1$ or k_2. Therefore, the rate constants of IsdA obtained from the time course in Fig. 3 are directly equal to $k_{-\text{hemin}}$ in Scheme 1.

The association equilibrium constants (K_{hemin}) for hemin binding to apo-IsdA can be estimated by the ratio of the apparent second-order association rate constant ($k'_{\text{hemin}} = k_{\text{coordination}}/K_d$) and the hemin dissociation rate constant $k_{-\text{hemin}}$. The K_{hemin} value for IsdA is 3.8×10^{11} M^{-1} (Table 1).

An attempt was also made to determine the affinity of IsdC for hemin. The spectral changes of the hemin/apo-IsdC mixture indicate that most of hemin already bound to IsdC when the first spectrum was recorded in a stopped-flow spectrophotometer (Fig. 2*B*). Because the reaction is too fast, the $k_{\text{coordination}}$ and K_d of hemin association with apo-IsdC could not be reliably measured. Unlike the reaction of holo-IsdA and apomyoglobin, the 3.2 μM holo-IsdC, 48 μM apomyoglobin mixture at 12 h after mixing had a spectrum that was still more close to that of holo-IsdC than to that of holomyoglobin (Fig. 3*B*), and $\Delta(A_{600}-A_{544})$ associated with the holo-IsdC/apomyoglobin reaction was 20% of the expected change (Fig. 3*C*). These results indicate that IsdC has higher affinity for hemin than both IsdA and H64Y/V68F myoglobin.

Hemin Transfer from IsdA to Apo-IsdC—We next tested whether IsdA transfers its hemin to apo-IsdC. Holo-IsdA (36 μM) and 47 μM apo-IsdC were incubated at room temperature for 2 min, and the two proteins were separated on a small DEAE column. SDS-PAGE analysis confirmed the separation of the two proteins (Fig. 4*A*). The normalized spectra of IsdA and IsdC before and after the reaction are shown in Fig. 4, *B* and *C*, respectively. The ratio of A_{406}/A_{280} of the treated IsdA was 29% that of the starting holo-IsdA. A_{406} is the absorption by the bound hemin, and A_{280} is mainly absorbance of the protein moiety. The lower A_{406}/A_{280} ratio of treated IsdA indicates that IsdA lost hemin in its reaction with apo-IsdC. Consistent with this result, holo-IsdC was present in treated IsdC based on the presence of the absorbance of bound hemin (Fig. 4*C*). Measurements of protein and hemin contents of these samples indicated that 90% of the holo-IsdA and 65% of the apo-IsdC lost and gained hemin, respectively. These results indicate that IsdA efficiently transfers its hemin to apo-IsdC.

Equilibrium Constant of the Holo-IsdA/Apo-IsdC Reaction—To demonstrate whether the hemin transfer reaction is reversible, 15 μM holo-IsdC was incubated with 56 μM apo-IsdA for 2 min, and the two proteins were separated as described above. Based on the spectra of the separated proteins (Fig. 5) and the extinction coefficients, 24% of holo-IsdC transferred hemin to apo-IsdA. Thus, the reaction is reversible. To estimate the equilibrium constant of this reversible reaction, 33 μM holo-IsdA was incubated with apo-IsdC at 12, 24, 48, 71, or 95 μM at room temperature (22 °C) for 20 min, and the two proteins were separated. The concentrations of apo- and holo-forms of each isolated protein were calculated using the corresponding extinction coefficients, which were then used to determine the concentrations of apo- and holo-forms of each protein in the reaction mixture on the assumption that the separation did not

TABLE 1
Rate and equilibrium constants for hemin binding to IsdA

Kinetic parameter	IsdA
k_2/k_1 or K_d (hemin binding)[a]	3.3 ± 0.7 μM
$k_{\text{coordinatioin}}$[a]	330 ± 27 s^{-1}
$k'_{\text{hemin}} \approx k_{\text{coordination}}/K_d$, apparent bimolecular rate constant at low [protein]	100 μM^{-1} s^{-1}
$k_{-\text{hemin}}$[b]	0.95 ± 0.02 h^{-1}
$K_{\text{hemin}} \approx k'_{\text{hemin}}/k_{-\text{hemin}}$	3.8 × 10^{11} M^{-1}

[a] The values of the parameters were derived from the fast phase of the reaction of hemin with apoIsdA at 25 °C in 20 mM Tris-HCl, pH 8.0, according to Scheme 1 and Equation 1.
[b] The hemin dissociation rate constant from holoIsdA was determined by the H64Y/V68F apomyoglobin assay.

shift the equilibrium. Fig. 6 represents the concentrations of holo-IsdA, apo-IsdA, and holo-IsdC as a function of initial [apo-IsdC]/[holo-IsdA]. Based on these data, the mean value ± S.D. of the equilibrium constant of the reaction was found to be 10 ± 5. The results indicate that the equilibrium is in favor of holo-IsdC formation, being consistent with the higher affinity of IsdC for hemin than IsdA.

Kinetics of Hemin Transfer from IsdA to Apo-IsdC—Although oxidized holo-IsdA and holo-IsdC have similar Soret absorption peaks, holo-IsdC does have higher absorbance than holo-IsdA in the region between 350 and 405 nm (Fig. 7*A*). Because holo-IsdA transfers its hemin to apo-IsdC, there should be increase in absorbance in the region of 350–405 nm during the transfer, and this increase could be used to determine the kinetics of the hemin transfer reaction. Thus, limited holo-IsdA was reacted with apo-IsdC at various concentrations in a stopped-flow spectrophotometer, and spectra were recorded over time. The absorbance in the region of 350–405 nm was indeed rapidly increased after mixing holo-IsdA and apo-IsdC (Fig. 7*B*). The difference in absorbance between 374 and 344 nm (A_{374}–A_{344}) was used to determine the kinetics of the transfer. A_{374}–A_{344} increases rapidly and fits a single exponential equation (Fig. 7*C*), resulting in an observed first-order rate constant (k_{obs}). The k_{obs} value depends hyperbolically on [apo-IsdC] (Fig. 7*D*).

An attempt was also made to kinetically characterize hemin transfer from holo-IsdC to apo-IsdA. However, the spectral change was too little to be monitored because the reverse reaction is not efficient. Thus, the kinetics of the reverse reaction could not be determined by the analysis used in the forward reaction. The data can be interpreted by a minimal model for hemin transfer from holo-IsdA to apo-IsdC given in Scheme 2. In this model, holo-IsdA forms a complex with apo-IsdC, and hemin is then reversibly and directly transferred to apo-IsdC to yield apo-IsdA:holo-IsdC, which is subsequently dissociated into apo-IsdA and holo-IsdC. The reversible reaction can be neglected under the conditions in Fig. 7. When the initial [apo-IsdC] is ≥5 [holo-IsdA] and k_{transfer} presumably ≪ k_1, k_2, and k_3, the hemin transfer from holo-IsdA to apo-IsdC is a pseudo first-order process. The observed rate constant, k_{obs}, is given by Equation 2,

$$k_{\text{obs}} = \frac{k_{\text{transfer}}[\text{apoprotein}]}{(k_2 + k_{\text{transfer}})/k_1 + [\text{apoprotein}]} \approx \frac{k_{\text{transfer}}[\text{apoprotein}]}{K_d + [\text{apoprotein}]} \quad \text{(Eq. 2)}$$

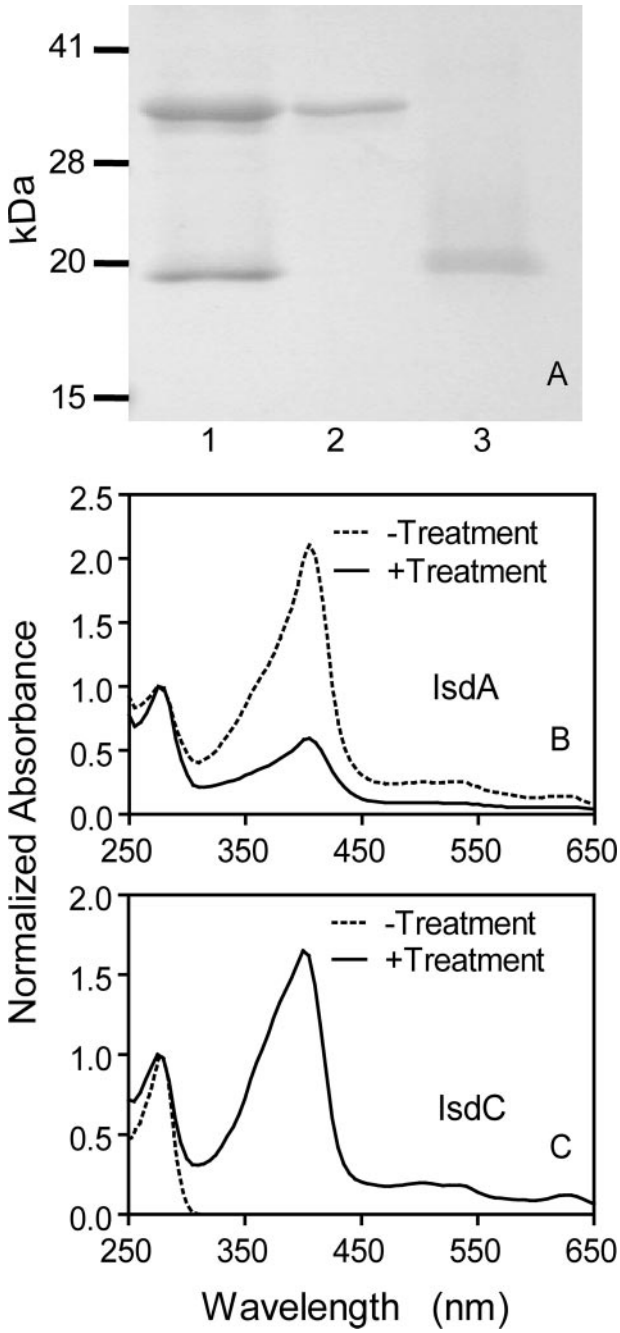

FIGURE 4. **Efficient hemin transfer from holo-IsdA to apo-IsdC.** Apo-IsdC (47 μM) was incubated with 36 μM holo-IsdA in 0.1 ml of 20 mM Tris-HCl, pH 8.0, at room temperature for 2 min. The two proteins were separated as described in the text. *A*, SDS-PAGE analysis showing separation of IsdA and IsdC from their mixture. *Lane 1*, holo-IsdA/apo-IsdC mixture before separation; *lane 2*, IsdA isolated from the mixture; *lane 3*, IsdC isolated from the mixture. *B*, spectra of holo-IsdA (*dashed curve*) and treated IsdA (*solid curve*). *C*, spectra of apo-IsdC (*dashed curve*) and treated IsdC (*solid curve*).

where K_d is the dissociation constant of the holo-IsdA-apo-IsdC complex, and k_1, k_2, and k_{transfer} are the rate constants of the individual reactions proposed in Scheme 2. Fitting of the data in Fig. 7*D* to Equation 2 yielded values of k_{transfer} and K_d equal to 54.3 ± 1.8 s^{-1} and 17 ± 1.3 μM, respectively (Table 2).

Activation Parameters for Hemin Transfers from IsdA to Apo-IsdC—To estimate the activation parameters for hemin transfer from IsdA to apo-IsdC, the values of k_{transfer} at different

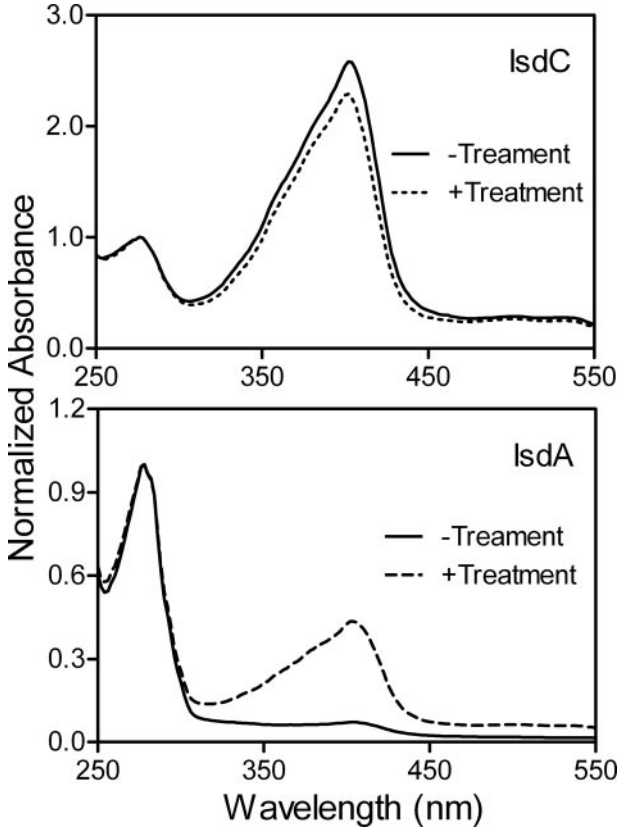

FIGURE 5. **Inefficient hemin transfer from holo-IsdC to apo-IsdA.** Apo-IsdA (56 μM) was incubated with 15 μM holo-IsdC in 0.1 ml of 20 mM Tris-HCl, pH 8.0, at room temperature for 2 min, and the two proteins were separated. Shown are the normalized spectra of IsdC (*A*) and IsdA (*B*) without and with the treatment.

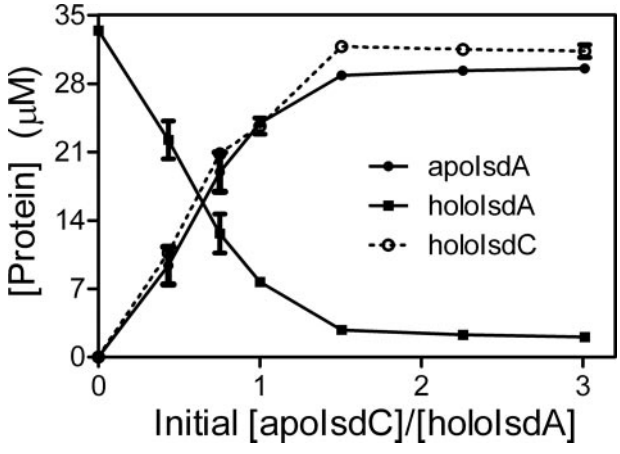

FIGURE 6. **Apo-IsdC titration in hemin transfer from holo-IsdA to apo-IsdC.** Holo-IsdA (33 μM) was incubated with 12, 24, 48, 71, or 95 μM apo-IsdC in 20 mM Tris-HCl, pH 8.0, at 22 °C for 20 min. Shown are the concentrations of holo-IsdA, apo-IsdA, and holo-IsdC in the mixtures as a function of the ratio of initial [apo-IsdC]/[holo-IsdA].

temperatures from 17 to 25 °C were determined as described above. The $k_{transfer}$ could not be measured at ≥30 °C because the reaction was too fast. The data were analyzed according to the Eyring equation (Equation 3).

$$\ln\frac{k}{T} = -\frac{\Delta H^{\ddagger}}{R}\left(\frac{1}{T}\right) + \ln\frac{k_B}{h} + \frac{\Delta S^{\ddagger}}{R} \qquad \text{(Eq. 3)}$$

where k_B, h, and R are Boltzman's, Planck's, and the gas constants, respectively. The values of the activation entropy ($\Delta S^{\ddagger}$) and enthalpy ($\Delta H^{\ddagger}$) for the first-order transfer of hemin were 15 ± 7 J/(K mol) and 67 ± 12 kJ/mol, respectively. The free energy of activation, $\Delta G^{\ddagger}$ calculated as $\Delta H^{\ddagger} - T\Delta S^{\ddagger}$, was 63 kJ/mol at 25 °C.

Enthalpy and Entropy Changes for Formation of the Holo-IsdA-Apo-IsdC Complex—The values of the equilibrium dissociation constant for formation of the transient holo-IsdA-apo-IsdC complex at different temperatures were also determined as described above and analyzed by the van't Hoff equation (Equation 4).

$$\ln K_{association} = -\frac{\Delta H^0}{R}\left(\frac{1}{T}\right) + \frac{\Delta S^0}{R} \qquad \text{(Eq. 4)}$$

where $K_{association}$ is the equilibrium association constant for formation of the holo-IsdA-apo-IsdC complex and equal to $1/K_d$ from Table 2. The standard enthalpy (ΔH^0) and entropy (ΔS^0) changes were −68 ± 11 kJ/mol and −136 ± 39 J/(K mol) for the formation of holo-IsdA:apo-IsdC, respectively. The standard free energy change, ΔG^0, is −27 kJ/mol for the formation of the holo-IsdA-apo-IsdC complex.

DISCUSSION

The Isd proteins have been extensively characterized in terms of their function in hemin acquisition, hemin binding, and structures of the proteins or heme-binding domains. However, little is known about the biochemical mechanism of the heme acquisition by the Isd system. In this study, we demonstrate the rapid, direct, and affinity-driven hemin transfer from IsdA to IsdC, documenting the first protein-to-protein hemin transfer in the Isd system and providing the first example of hemin transfer from one surface protein to another surface protein in Gram-positive bacteria. In addition, the kinetic and thermodynamic analyses suggest that the hemin transfer is through an activated holo-IsdA-apo-IsdC complex.

Apo-IsdA and holo-IsdC are formed during the brief incubation of holo-IsdA with apo-IsdC. The spectrum of the holo-IsdA/apo-IsdC mixture shifts from the spectrum of holo-IsdA to that of holo-IsdC. Thus, holo-IsdA and apo-IsdC lose and gain hemin, respectively, during the incubation of holo-IsdA with apo-IsdC, and the spectral change can be used to follow the hemin transfer.

Kinetic analyses of the transfer and hemin dissociation from holo-IsdA strongly indicate that holo-IsdA directly transfers its hemin to apo-IsdC. In indirect transfer, hemin is first dissociated into solvent from the donor and then captured by the acceptor. If the IsdA-to-IsdC hemin transfer were indirect, the rate of the transfer should be close to the rate of the hemin dissociation from IsdA. However, the rate constant of the transfer is >70,000 times greater than the rate of simple hemin dissociation from holo-IsdA into solvent ($k_{transfer}$ = 54.3 s^{-1} *versus* k_{-hemin} = 0.00076 s^{-1}), ruling out an indirect transfer mechanism. Furthermore, the values of observed $k_{transfer}$ depend hyperbolically on [apo-IsdC]. This result indicates that holo-IsdA forms a complex with apo-IsdC prior to hemin transfer, further supporting a direct transfer mechanism.

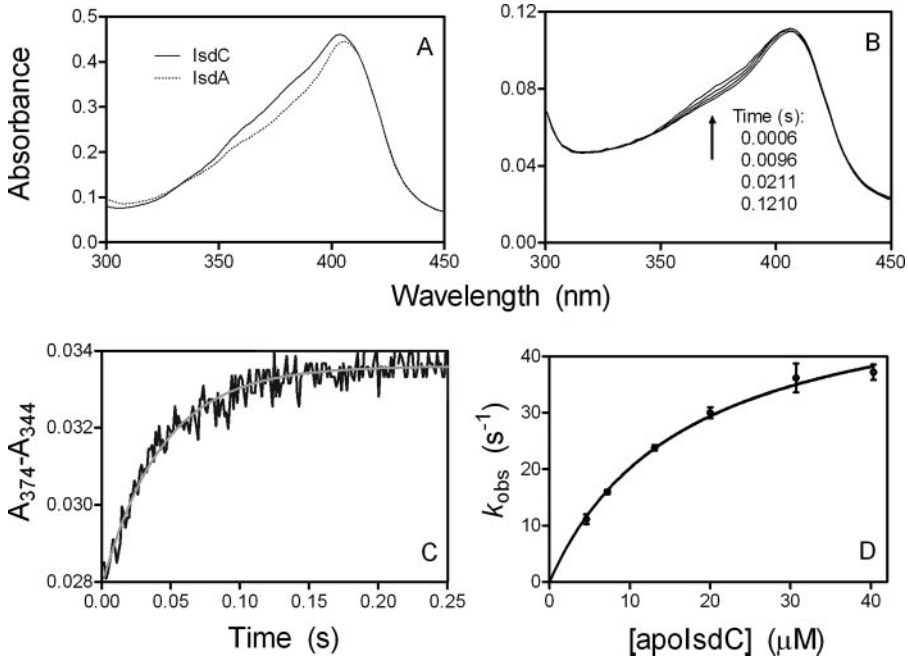

FIGURE 7. **Spectral evidence for and kinetics of direct hemin transfer from holo-IsdA to apo-IsdC.** *A*, comparison of the spectra of 4.5 μM holo-IsdA and holo-IsdC in 20 mM Tris-HCl, pH 8.0. *B*, absorption spectra of a mixture of 1.3 μM holo-IsdA and 7.4 μM apo-IsdC as a function of time after mixing in a stopped-flow spectrophotometer. *C*, time course of A_{374}–A_{344} for the reaction in *B*. The *black trace* and *gray curve* represent the observed data and single exponential fitting curve, respectively. *D*, observed rate constant plotted as a function of [apo-IsdC]. The rate constants at different [apo-IsdC] were obtained from single exponential fitting as in *C*, and the *curve* is the theoretical curve obtained by fitting the data to Equation 2.

$$\text{holoIsdA} + \text{apoIsdC} \underset{k_2}{\overset{k_1}{\rightleftharpoons}} \text{holoIsdA-apoIsdC} \underset{k_{-transfer}}{\overset{k_{transfer}}{\rightleftharpoons}} \text{apoIsdA-holoIsdC} \underset{k_4}{\overset{k_3}{\rightleftharpoons}} \text{apoIsdA} + \text{holoIsdC}$$

SCHEME 2

TABLE 2

Comparison of rate constants and activation parameters for hemin transfer in the holoIsdA/apoIsdC and holoShp/apoHtsA reactions

Kinetic parameter	HoloIsdA/apoIsdC	HoloShp/apoHtsA
k_2/k_1 or K_d [a]	17 ± 1.3 μM	48 ± 7 μM
$k_{transfer}$ [a]	54.3 ± 1.8 s^{-1}	43 ± 3 s^{-1}
$\Delta H^0_{complex}$ [b,c]	−68 ± 11 kJ/mol	−37 ± 6 kJ/mol
$\Delta S^0_{complex}$ [b,d]	−136 ± 39 J/mol K	−37 ± 18 J/mol K
$\Delta G^0_{complex}$ [b,d]	−27 kJ/mol	−26 kJ/mol
$\Delta S^{\ddagger}$ for $k_{transfer}$ [c,d]	15 ± 7 J/mol K	35 ± 4 J/mol K
$\Delta H^{\ddagger}$ for $k_{transfer}$ [c,d]	67 ± 12 kJ/mol	75 ± 9 kJ/mol
$\Delta G^{\ddagger}$ for $k_{transfer}$ [c,d]	63 kJ/mol	64.9 kJ/mol
$k_{transfer}/K_d$, apparent bimolecular rate constant at low [protein]	3.2 μM^{-1} s^{-1}	0.8 μM^{-1} s^{-1}

[a] The values for k_2/k_1 and $k_{transfer}$ at 25 °C in 20 mM Tris-HCl, pH 8.0, were obtained from fits of the dependence of the observed rate constants of transfer on [apoprotein] to Equation 2.

[b] The standard entropy, enthalpy, and free energy for the formation of the holoIsdA-apoIsdC complexes were obtained by analyzing the dependence of $K_{association}$ ($1/K_d$) on temperature according to the van't Hoff plot.

[c] The activation entropy, enthalpy, and free energy were obtained by analyzing the dependence of $k_{transfer}$ on temperature according to the Eyring equation.

[d] The data for the holoShp/apoHtsA reaction were from Ref. 14.

Because hemin aggregates in aqueous solution, it has been a challenge to estimate the affinity of hemoproteins for hemin using kinetic analysis of hemin association to apoproteins and dissociation from holoproteins. The secondary order rate constants of hemin association have been estimated as the rate constants of association of CO-heme complex with apoproteins (32). The accuracy of this estimation is unknown. Thus, we performed the kinetic analysis of hemin association with apo-IsdA, which fits a two-exponential equation with ~70% of spectral change attributable to the fast phase. de Villiers *et al.* (30) recently reported that aqueous hemin solution contains only monomers and dimers. Using the method of de Villiers *et al.* (30), percentile of monomeric hemin in the hemin solution before mixing with apo-IsdA in our stopped-flow measurements was estimated to be ~60%. Our data could be interpreted as follows. The fast phase is the reaction of monomeric hemin with apo-IsdA, whereas the slower phase is the dissociation of dimeric hemin followed by the rapid association of the resulting monomeric hemin with apo-IsdA. Thus, we could use the fast phase of the reaction to obtain the secondary rate constant of the hemin association to apo-IsdA.

Although we can estimate the affinity of IsdA for hemin, the affinity of IsdC for hemin could not be determined under the same conditions, because the values of $k_{coordination}$ in hemin association and k_{-hemin} in hemin dissociation could not be determined. However, our data strongly indicate that IsdC has a much higher affinity for hemin than IsdA. First, hemin association to apo-IsdC is faster than that to apo-IsdA. Second, the majority of hemin in holo-IsdA, but not holo-IsdC, was lost to the apomyoglobin under the same conditions. Third, the hemin transfer from holo-IsdA to apo-IsdC is reversible, and the equilibrium constant of the reaction is about 10 in favor of holo-IsdC formation. If the interaction between IsdA and IsdC does not shift the equilibrium, IsdC would have an affinity for hemin 10-fold as that of IsdA. The Trp-77 residue unique to IsdC "interlocks" hemin into its pocket in its crystal structure, and this effect has been proposed to account for assumed higher hemin affinity of IsdC *versus* that of all other Isd proteins containing the NEAT domain(s) (20). Our data are consistent with this hypothesis but also suggest that the faster rate of hemin association to apo-IsdC also contributes to the higher affinity of IsdC for hemin. Taken together, our data indicate that efficient hemin transfer from IsdA to IsdC is at least partially driven by the higher affinity of IsdC for hemin compared with that of IsdA.

It has previously been hypothesized that hemin is transferred in the following order: IsdH-haptoglobin-hemoglobin/IsdB-hemoglobin → IsdA → IsdC → IsdDEF and/or HtsABC (25, 26). Rapid and direct hemin transfer from IsdA to IsdC provides the first piece of experimental evidence supporting this hypothesis. It will be necessary to examine hemin transfer reactions and kinetic mechanisms for the various protein couples of these

TABLE 3
Comparison of apparent rate and equilibrium constants for hemin binding to apoIsdA, apoIsdC, and other hemin protein complexes

Heme protein	k'_{hemin}	k_{-hemin}	K_{hemin}	Ref.
	$\mu M^{-1} s^{-1}$	s^{-1}	M^{-1}	
ApoIsdA				
Without apoIsdC	100	0.00026	3.8×10^{11}	This work
With apoIsdC		54.3		
ApoIsdC			$\sim 3.8 \times 10^{12}$ [a]	This work
ApoShp				14
Without apoHtsA	1.6	0.0003	5×10^{9}	
With apoHtsA		43		
ApoHtsA	80	0.0026	3.1×10^{10}	14
Hemophore HasA			5.3×10^{10}	31
Human apohemoglobin				33
α (tetramers)	~100	0.00008	$\sim 1.2 \times 10^{12}$	
α (dimers)	~100	0.00016	$\sim 6 \times 10^{11}$	
α (monomers)	~100	0.0033	$\sim 3.3 \times 10^{10}$	
β (tetramers)	~100	0.00041	$\sim 2.5 \times 10^{11}$	
β (dimers)	~100	0.0042	$\sim 2.4 \times 10^{10}$	
β (monomers)	~100	0.011	$\sim 9 \times 10^{9}$	

[a] Data were estimated from the value of K_{hemin} of IsdA and the equilibrium constant ($K_{eq} = 10$) of the reaction of holoIsdA with apoIsdC on the assumption that the K_{eq} value is solely dependent on the relative affinity of IsdA and IsdC for hemin.

proteins to fully establish a heme acquisition model in the Isd system.

The Shr/Shp/HtsABC and Isd systems are two distinct heme acquisition pathways composed of surface proteins and ABC transporter in Gram-positive pathogens. Shr likely binds host hemoproteins (7) and has two NEAT domains (17). The protein binds hemin and transfers it to apo-Shp but not to apo-HtsA (16). Although Shp was not included in the NEAT family by Andrade *et al.* (17), the homology in amino acid sequence between the heme-binding domain of Shp and the heme-binding or NEAT domain of IsdA or IsdC (17–19% identity) is similar to that between the IsdA and IsdC NEAT domains (19% identity) (18), suggesting that Shp is at least a distant member of the NEAT family that includes Shr, IsdH, IsdA, IsdB, and IsdC (17). We have shown that Shp rapidly and directly transfers its hemin to apo-HtsA. These observations suggest a heme flow model of hemoglobin → Shr → Shp → HtsA in the *S. pyogenes* system. It appears that there are parallel functions of the components in the two systems, *i.e.* Shr functions like IsdH/B, Shp like IsdA/C, and HtsA like IsdE and/or *S. aureus* HtsA.

The affinities of IsdA and IsdC for hemin are greater than those of Shp and HtsA (Table 3). IsdA-hemin and IsdC-hemin complexes are pentacoordinate and use Tyr as their only axial ligand (19, 20), whereas Shp- and HtsA-hemin complexes are hexacoordinate using two Met and Met/His residues as the axial ligands, respectively (15, 18). The Tyr-hemin ligation may be a major factor for the higher hemin affinities of IsdA and IsdC. The axial Met residues of the Shp heme iron are both required for rapid Shp-to-HtsA hemin transfer (15), and the hemin acceptor in each couple has a higher affinity for hemin, suggesting that the axial ligands and relative hemin affinity may have been evolved for efficient hemin transfer in each system.

IsdA apparently transfers its hemin to apo-IsdC through an activated transfer mechanism. Holo-IsdA forms a complex with apo-IsdC, releasing free energy. The free energy released is used to weaken hemin binding in holo-IsdA and thus facilitate transfer to apo-IsdC. This mechanism is similar to that of hemin and heme transfer from streptococcal Shp to apo-HtsA (14). Protein interaction also is critical for hemin transfer from *Serratia marcescens* hemophore HasA to HasA receptor HasR (1). The mechanism of activated heme transfer may apply in general to all direct heme transfers in bacterial heme transport systems.

Acknowledgments—We thank Drs. John Olsen and Mark Quinn for critical reading of the manuscript.

REFERENCES

1. Izadi-Pruneyre, N., Huche, F., Lukat-Rodgers, G. S., Lecroisey, A., Gilli, R., Rodgers, K. R., Wandersman, C., and Delepelaire, P. (2006) *J. Biol. Chem.* **281,** 25541–25550
2. Burkhard, K. A., and Wilks, A. (2007) *J. Biol. Chem.* **282,** 15126–15136
3. Klebba, P. E., Rutz, J. M., Liu, J., and Murphy, C. K. (1993) *J. Bioenerget. Biomemb.* **25,** 603–611
4. Griffiths, E., and Williams, P. (1999) in *Iron and infection: Molecular, Physiological, and Clinical Aspects* (Bullen, J. J., and Griffiths, E., eds), pp. 87–212, John Wiley & Sons, Inc., Chichester, UK
5. Drazek, E. S., Hammack, C. A., and Schmitt, M. P. (2000) *Mol. Microbiol.* **36,** 68–84
6. Lei, B., Liu, M., Voyich, J. M., Prater, C. I., Kala, S. V., DeLeo, F. R., and Musser, J. M. (2003) *Infect. Immun.* **71,** 5962–5969
7. Bates, C. S., Montanez, G. E., Woods, C. R., Vincent, R. M., and Eichenbaum, Z. (2003) *Infect. Immun.* **71,** 1042–1055
8. Skaar, E. P., Humayun, M., Bae, T., DeBord, K. L., and Schneewind, O. (2004) *Science* **305,** 1626–1628
9. Nygaard, T. K., Liu, M., McClure, M. J., and Lei, B. (2006) *BMC Microbiol.* 6:82
10. Lei, B., Smoot, L. M., Menning, H., Voyich, J. M., Kala, S. V., Deleo, F. R., and Musser, J. M. (2002) *Infect. Immun.* **70,** 4494–4500
11. Mazmanian, S. K., Skaar, E. P., Gaspar, A. H., Humayun, M., Gornicki, P., Jelenska, J., Joachmiak, A., Missiakas, D. M., and Schneewind, O. (2003) *Science* **299,** 906–909
12. Maresso, A. W., Chapa, T. J., and Schneewind, O. (2006) *J. Bacteriol.* **188,** 8145–8152
13. Liu, M., and Lei, B. (2005) *Infect. Immun.* **73,** 5086–5092
14. Nygaard, T. K., Blouin, G. C., Liu, M., Fukumura, M., Olson, J. S., Fabian, M., Dooley, D. M., and Lei, B. (2006) *J. Biol. Chem.* **281,** 20761–20771
15. Ran, Y., Zhu, H., Liu, M., Fabian, M., Olson, J. S., Aranda, R., IV, Phillips, G. N., Jr., Dooley, D. M., and Lei, B. (2007) *J. Biol. Chem.* **282,** 31380–31388
16. Zhu, H., Liu, M., and Lei, B. (2008) *BMC Microbiol.* 8:15
17. Andrade, M. A., Ciccarelli, F. D., Perez-Iratxeta, C., and Bork, P. (2002) *Genome Biol.* **3,** research0047
18. Aranda, R., Worley, C. E., Liu, M., Bitto, E., Cates, M. S., Olson, J. S., Lei, B., and Phillips, G. N., Jr. (2007) *J. Mol. Biol.* **374,** 374–383
19. Grigg, J. C., Vermeiren, C. L., Heinrichs, D. E., and Murphy, M. E. (2007) *Mol. Microbiol.* **63,** 139–149
20. Sharp, K. H., Schneider, S., Cockayne, A., and Paoli, M. (2007) *J. Biol. Chem.* **282,** 10625–10631
21. Torres, V. J., Pishchany, G., Humayun, M., Schneewind, O., and Skaar, E. P. (2006) *J. Bacteriol.* **188,** 8421–8429
22. Dryla, A., Gelbmann, D., von Gabain, A., and Nagy, E. (2003) *Mol. Microbiol.* **49,** 37–53
23. Mack, J., Vermeiren, C., Heinrichs, D. E., and Stillman, M. J. (2004) *Biochem. Biophys. Res. Commun.* **320,** 781–788
24. Vermeiren, C. L., Pluym, M., Mack, J., Heinrichs, D. E., and Stillman, M. J. (2006) *Biochemistry* **45,** 12867–12875
25. Maresso, A. W., and Schneewind, O. (2006) *Biometals* **19,** 193–203
26. Reniere, M. L., Torres, V. J., and Skaar, E. P. (2007) *Biometals* **20,** 333–345
27. Ascoli, F., Fanelli, M. R., and Antonini, E. (1981) *Methods Enzymol.* **76,** 72–87
28. Fuhrhop, J. H., and Smith, K. M. (1975) in *Porphyrins and Metalloporphy-*

rins (Smith, K. M., ed), pp. 804–807, Elsevier Publishing Co., New York
29. Hargrove, M. S., Singleton, E. W., Quillin, M. L., Ortiz, L. A., Phillips Jr., G. N., Olson, J. S., and Mathews, A. J. (1994) *J. Biol. Chem.* **269,** 4207–4214
30. de Villiers, K. A., Kaschula, C. H., Egan, T. J., and Marques, H. M. (2007) *J. Biol. Inorg. Chem.* **12,** 101–117
31. Deniau, C., Gilli, R., Izadi-Pruneyre, N., Létoffé, S., Delepierre, M., Wandersman, C., Briand, C., and Lecroisey, A. (2003) *Biochemistry* **42,** 10627–10633
32. Hargrove, M. S., Barrick, D., and Olson, J. S. (1996) *Biochemistry* **35,** 11293–11299
33. Hargrove, M. S., Whitaker, T., Olson, J. S., Vali, R. J., and Mathews, A. J. (1997) *J. Biol. Chem.* **272,** 17385–17389

Direct Hemin Transfer from IsdA to IsdC in the Iron-regulated Surface Determinant (Isd) Heme Acquisition System of *Staphylococcus aureus*

Mengyao Liu, Wesley N. Tanaka, Hui Zhu, Gang Xie, David M. Dooley and Benfang Lei

J. Biol. Chem. 2008, 283:6668-6676.
doi: 10.1074/jbc.M708372200 originally published online January 9, 2008
